The Drosophila *slamdance* Gene: A Mutation in an Aminopeptidase Can Cause Seizure, Paralysis and Neuronal Failure

HaiGuang Zhang,*[,1] Jeff Tan,*[,1] Elaine Reynolds,[†] Daniel Kuebler,* Sally Faulhaber* and Mark Tanouye*[,‡,2]

**Department of Molecular and Cell Biology, Division of Neurobiology, [‡]Department of Environmental Science, Policy, and Management, Division of Insect Biology, University of California, Berkeley, California 94720 and [†]Department of Biology, Lafayette College, Easton, Pennsylvania 18042*

Manuscript received February 20, 2002
Accepted for publication August 15, 2002

ABSTRACT

We report here the characterization of *slamdance* (*sda*), a *Drosophila melanogaster* "bang-sensitive" (BS) paralytic mutant. This mutant exhibits hyperactive behavior and paralysis following a mechanical "bang" or electrical shock. Electrophysiological analyses have shown that this mutant is much more prone to seizure episodes than normal flies because it has a drastically lowered seizure threshold. Through genetic mapping, molecular cloning, and RNA interference, we have demonstrated that the *sda* phenotype can be attributed to a mutation in the Drosophila homolog of the human aminopeptidase N (APN) gene. Furthermore, using mRNA *in situ* hybridization and LacZ staining, we have found that the *sda* gene is expressed specifically in the central nervous system at particular developmental stages. Together, these results suggest that the bang sensitivity in *sda* mutants is caused by a defective APN gene that somehow increases seizure susceptibility. Finally, by using the *sda* mutation as a sensitized background, we have been able to identify a rich variety of *sda* enhancers and other independent BS mutations.

MEMBRANE peptidases are a group of ectoenzymes that are widely distributed in animal tissues and have been implicated in a variety of biological functions. They have been shown to be essential for maturation of proteins, activation and inactivation of hormonal peptides, degradation of nonhormonal peptides, and determination of protein stability. They can also function as receptors and as molecules involved in cell adhesion and signal transduction (Sanderink *et al.* 1988; Taylor 1993). Aminopeptidase N (APN; EC 3.4.11.2) is a transmembrane ectoenzyme that catalyzes the removal of neutral and basic amino acids from the N termini of a number of small peptide substrates (Shipp and Look 1993; Riemann *et al.* 1999). The catalytic domain faces the exterior of the plasma membrane and is anchored by a transmembrane-spanning domain. Human APN is identical to CD13, a cluster antigen expressed on the surface of myeloid progenitors, monocytes, granulocytes, and myeloid leukemia cells (Look *et al.* 1989). Depending on the species, the APN protein is composed of 963–967 amino acids with a short N-terminal tail in the cytoplasm (9–10 amino acids), a transmembrane segment (23- to 24-amino-acid residues), and a large extracellular ectodomain containing the active site (Luciani *et al.* 1998). APN is a member of the M_1 family of zinc-dependent metallopeptidases, which includes related enzymes such as aminopeptidase A, aminopeptidase B, leukotriene A4 hydrolase, puromycin-sensitive aminopeptidase, thyrotropin-releasing hormone-degrading enzyme, the rat vesicle protein Vp 165, and *Escherichia coli* pepN (McCaman and Gabe 1986; Funk *et al.* 1987; Schauder *et al.* 1991; Nanus *et al.* 1993; Constam *et al.* 1995; Keller *et al.* 1995; Rawlings and Barrett 1995; Fukasawa *et al.* 1996; Cadel *et al.* 1997).

APN is highly expressed in liver, brush borders of kidney, small intestine, and placenta (Shipp and Look 1993; Riemann *et al.* 1999). It has also been found in the brain, lung, blood vessels, and primary cultures of fibroblasts. APN has been implicated in a variety of tissue-specific functions. In the intestinal brush border, APN functions in the final hydrolysis of ingested nutrients and in amino acid scavenging. On vascular cells, APN serves to metabolize particular vasoactive peptides (Ward *et al.* 1990). In malignant neoplasms, APN is widely considered to influence the invasion mechanism by catalyzing the degradation of collagen type IV and enabling tumor-cell invasion through the basement membrane during metastasis of a primary tumor to vital organs (Saiki *et al.* 1993; Kido *et al.* 1999; Ishii *et al.* 2001). APN is thought to play a role in antigen processing and presentation (Falk *et al.* 1994). Cell cycle control and cell differentiation of macrophages/monocytes and mitogenic activation of lymphocytes are also associated with surface APN activity (Amoscato *et al.* 1989; Koch *et*

Sequence data from this article have been deposited with the EMBL/GenBank Data Libraries under accession no. AF480087.

[1]These authors contributed equally to this work.

[2]*Corresponding author:* Department of Environmental Science, Policy, and Management, 201 Wellman Hall, University of California, Berkeley, CA 94720. E-mail: tanouye@uclink4.berkeley.edu

al. 1991). APN appears to be directly linked to signal transduction pathways in monocytes by mediating the release of Ca^{2+} from intracellular stores and the extracellular milieu (Santos *et al.* 2000). In humans, APN is thought to act as a receptor for coronavirus 229E and it is a receptor for transmissible gastroenteritis virus in pig (Delmas *et al.* 1992, 1994; Yeager *et al.* 1992). In the brain, APN is involved in the enzymatic cascade of the renin-angiotensin system through the cleavage of angiotensin III (Zini *et al.* 1996). In synaptic membranes, it is widely believed to play the principal role in the inactivation of enkephalin signaling by catalyzing the release of N-terminal tyrosine from the peptide (Solhonne *et al.* 1987). In mouse brain cortical slices, APN appears to be associated with the metabolism of nociceptin/orphanin FQ, the natural ligand for the nucleolus organizing region (NOR) receptor (Montiel *et al.* 1997; Terenius *et al.* 2000). Thus, these studies show that in a variety of different tissues, APN displays an amazing diversity of physiological functions.

In this study, we present evidence for a novel APN function: a role in behavior and nervous system excitability as revealed by Drosophila mutants. One class of behavioral mutants, the "bang-sensitive" (BS) mutant class, has especially intriguing behavioral and electrophysiological phenotypes. The BS class includes several mutants such as *bangsenseless* (*bss*), *easily shocked* (*eas*), *slamdance* (*sda*), and *technical knockout* (*tko*). All BS mutants suffer from cycles of intense behavioral hyperactivity and temporary paralysis caused by a mechanical shock, such as a tap of the culture vial on the bench top or brief vortex mixing (a "bang"; Benzer 1971; Ganetzky and Wu 1982). The hyperactivity phenotype is characterized by intense, uncoordinated motor activity featuring wing flapping, leg shaking, and abdominal muscle contractions; the paralytic phenotype, on the other hand, is observed as a cessation of all physical activity (Benzer 1971; Pavlidis *et al.* 1994). The hyperactivity and paralysis can be mimicked on the electrophysiological level by stimulating and recording from the central nervous system (CNS; Pavlidis and Tanouye 1995; Kuebler and Tanouye 2000). These analyses show that BS mutants have enhanced seizure sensitivity, being 5–10 times more sensitive to seizures than wild-type flies.

So far, only two BS genes have been fully characterized: *tko*, which encodes a mitochondrial protein, and *eas*, which encodes an ethanolamine kinase (Royden *et al.* 1987; Pavlidis *et al.* 1994). In this article we present findings from two lines of study on *sda*, a previously uncharacterized BS mutant. First, we report the results of behavioral and electrophysiological testing on adult *sda* flies, which shows that *sda* mutants have a dramatically reduced seizure threshold compared to wild-type flies. We then present genetic and molecular data that suggest a mutation in the structural gene for a Drosophila homolog of human APN is responsible for the bang sensitivity in *sda* mutants. *In situ* hybridization and LacZ staining reveal *sda* gene expression, most notably in the CNS. Finally, we describe the results of a genetic screen in which the *sda* mutation was used to generate a sensitized genetic background: We were able to obtain various enhancers of *sda* as well as other independent BS mutations. Since it is surprising that a modification in an APN gene can alter neuronal excitability, our analysis of *sda* may encourage new ways of thinking about factors influencing seizure sensitivity.

MATERIALS AND METHODS

Fly stocks and genetic mapping of *sda*: Stocks were maintained on standard cornmeal-molasses medium at 22°. Wild-type flies were the Canton-Special (CS) strain. Three BS mutants were used: *eas*, *bss*, and *sda*. The *eas* gene is located at map position 1-53.5 and encodes an ethanolamine kinase (Pavlidis *et al.* 1994). The *bss* gene is located at 1-54.6; its gene product has not been described (Ganetzky and Wu 1982). The mutant *sda* allele, $sda^{iso7.8}$, was identified by Dr. Tim Tully (Cold Spring Harbor Laboratory) as a spontaneous mutation that caused behavioral paralysis following a mechanical bang stimulus; it was provided to us as a generous gift. The *sda* gene was mapped to an apparent map position of 3-95.9 on chromosome 3R on the basis of recombination relative to *ebony* (*e*), *rough* (*ro*), and *claret* (*ca*) markers. Cytogenetic analysis placed the *sda* locus within a five-band region (97D1–5) on the basis of its inclusion in the deficiencies *Df(3R)ro-XB3 = Df(3R) 97D1-2; 97D9* and *Df(3R)ro-z1 = Df(3R) 97D1-2; 97D15* and its exclusion from *Df(3R)Bd = Df(3R) < 97D5; 97F1-98A1.*

Isolation of the $sda^{HZ.P1}$ mutation: The $sda^{HZ.P1}$ allele was isolated in a screen utilizing *P*-element hybrid dysgenesis. It is a recessive lethal of *sda* that fails to complement the behavioral paralysis phenotype of $sda^{iso7.8}$. The $sda^{HZ.P1}$ mutation was isolated in a cross utilizing *ry* $P(ry^+$ *LacZ)(97D6-9)/ry Sb* $P(ry^+$ *delta2.3)* females crossed with *ry* $sda^{iso7.8}$ males. These females contain a *P* element located at 97D6–9, close to the map position of $sda^{iso7.8}$ that might facilitate mutation of *sda* by local hopping. The starting transposon insert itself does not cause BS phenotypes and complements $sda^{iso7.8}$. The female is dysgenic due to the overproduction of transposase by the $P(ry^+$ *delta2.3)*. Exceptional *ry* $P(ry^+$ *LacZ)(97D6-9)/ry* $sda^{iso7.8}$ male and female progeny from this cross that show bang-sensitive paralysis are individually crossed to set up appropriate stocks. The screen examined 20,000 flies, and two mutations were identified, one of which, $sda^{HZ.P1}$, failed to complement $sda^{iso7.8}$. Both the lethality and the failure to complement paralysis phenotypes reverted when the *P* element of $sda^{HZ.P1}$ was lost upon remobilization. The transposon of $sda^{HZ.P1}$ was mapped to 97D2–8 by *in situ* hybridization to polytene salivary gland chromosomes. The $sda^{HZ.P1}$ and $sda^{iso7.8}$ mutations are tightly linked and recombination experiments have not been able to separate them: Among 800 progeny of heterozygous females, no wild-type recombinants were identified.

Isolation of dominant enhancer mutations for $sda^{iso7.8}$/+: Dominant enhancer mutations of an $sda^{iso7.8}$/+ paralytic phenotype were identified in a screen utilizing *P*-element hybrid dysgenesis. Enhancers were isolated in a mating of *X^X,8:P(w*$^+$ *LacZ)/Y; ry Sb P(ry*$^+$ *delta2.3)/+* females crossed to *w/Y;* $sda^{iso7.8}$ males. These females contain an attached-X chromosome with eight mobile *P*-element transposons, each marked with w^+ and containing a LacZ reporter, an origin of replication, and an ampicillin-resistance gene to allow cloning via plasmid res-

cue. The females are dysgenic due to the overproduction of transposase by the *P(ry^{+} delta2.3)*. Exceptional *w/Y; sda$^{iso7.8}$/+* male progeny that showed bang-sensitive paralysis were individually crossed to set up appropriate stocks. Of 12,000 flies examined, 15 were bang sensitive. Linkage to the second or third chromosome was determined by segregation using *T(2;3)ap^{Xa}* and *Cyo* and *TM3* balancers. Six mutations segregated with the second chromosome and nine segregated with the third chromosome.

Behavioral testing: Testing for BS paralysis was performed on flies 2–3 days posteclosion. Flies were rested for >2 hr after exposure to CO_2 anesthesia before testing. Ten flies were then placed into a clean vial (Applied Scientific) and allowed to rest for an additional 30 min. These flies were vortexed on a VWR vortex at maximum setting for 10 sec and for those flies that showed paralysis, the recovery process was monitored. To test for refractory period, the flies were vortexed again 4–20 min later to see if the flies were still bang sensitive. To minimize data variation due to experimental setting or handling, a large number of flies ($n > 100$) were analyzed for each strain in this study.

Electrophysiology: Electrophysiology was performed on flies 2–3 days posteclosion using methods previously described to stimulate and record giant fiber (GF)-driven muscle potentials and seizures (Kuebler and Tanouye 2000). In brief, the fly was taken from a vial by sucking onto its head with a 23-gauge needle attached to a vacuum line. Another needle attached to a vacuum line was used to suck onto the abdomen, thereby completely immobilizing the fly. The fly was then affixed to a mounting needle by cyanoacrylate adhesive. Two types of stimulation were delivered to the brain, using bipolar tungsten stimulating electrodes: single-pulse stimuli and high-frequency (HF) wavetrains. Single-pulse stimuli (0.5 msec duration, 0.8 Hz) were used to drive the GF. GF-driven muscle potentials were recorded from the dorsal longitudinal muscles (DLMs), using tungsten recording electrodes. GF thresholds were determined as the lowest voltage at which the short-latency GF pathway responded. During the course of each experiment, the GF was stimulated continuously to assess GF system circuit function. To elicit seizures, short wavetrains of HF electrical stimuli (0.5-msec pulses delivered at 200 Hz for 300 msec) were delivered to the brain and the intensity (voltage) of the HF stimulus was varied as noted. Previously, we have shown that seizures in many genotypes, including *sda$^{iso7.8}$*, are elicited in an all-or-nothing manner (Kuebler and Tanouye 2000). Seizures consist of high-frequency activity in at least seven different muscle groups and >30 muscle fibers in the thorax. The activity in each muscle fiber corresponds to seizure activity in the motoneuron that innervates it. In this article, recordings of DLM muscle potentials were used to denote the occurrence of seizures as described previously (Kuebler and Tanouye 2000).

Molecular mapping of *sda*: Standard molecular techniques were employed for the manipulation of DNA and RNA (Sambrook *et al.* 1989). Molecular access to the *sda* region was achieved via plasmid rescue of genomic DNA from the *P*-element insertion in *sda$^{HZ.P1}$* (Wilson *et al.* 1989). Genomic DNA (2–5 μg) was digested with *Xba*I alone or in combination with either *Spe*I or *Nhe*I, and the fragments were self ligated with T_4 DNA ligase. Ligated products were transformed into *JS5* electrocompetent cells (Bio-Rad, Hercules, CA) and the transformants were selected on kanamycin (10 mg/ml) plates plus X-Gal and isopropyl thiogalactoside (IPTG). Plasmid DNA from positive clones (kan^{r}, LacZ+) was isolated, cut with restriction enzymes, and the fragments were used to probe Southern blots and Northern blots. The intron-exon boundaries of the *sda* gene were determined by sequencing the cDNA clone LP 11029 (Berkeley *Drosophila* Genome Project) and aligning the results to sequences in the genome database.

Analysis of mutant sequences: To examine the molecular basis of the *sda$^{iso7.8}$* mutation, PCR primers were designed to amplify the coding region of the *sda* gene in wild-type and mutant flies in six overlapping sections. The predicted products corresponded to the following nucleotide positions: primer set one, 477–1304; primer set two, 1199–2039; primer set three, 1648–2488; primer set four, 2270–3116; primer set five, 2803–3767; and primer set six, 3223–4031. These primers were used to amplify the *sda* coding sequence by reverse-transcribed PCR using adult whole RNA. The PCR products were cloned into TOPO vectors and sequenced (Invitrogen, San Diego). The insertion mutation in *sda$^{iso7.8}$* (contained within the PCR product of primer set one) was confirmed by sequencing at least two subclones of reverse-transcribed (RT)-PCR reactions. Other regions were also sequenced at least twice. The insertion site of the P allele, *sda$^{HZ.P1}$*, was determined by first using plasmid rescue to isolate the genomic fragment flanking the insertion site and then sequencing this fragment using a primer complementary to a site near the end of the *P*-element sequence (ATACTTCGGTAAGCTTCGGC).

Northern blots: For the developmental Northern blot, whole RNA was extracted from wild-type (*w^{1118}*) embryos (0–24 hr), third instar larvae, and adults, using Trizol reagent (GIBCO BRL, Gaithersburg, MD). The RNA was separated on a denaturing gel, blotted onto nitrocellulose membrane, and probed with radiolabeled DNA fragments using standard molecular biology techniques. The probe used here was an 848-bp fragment covering base pairs 62–908 of the *sda* gene sequence; labeling was done with [α-^{32}P]dCTP [New England Nucleotides, Stratagene (La Jolla, CA) Prime-It kit]. To compare *sda$^{iso7.8}$* mutants to wild-type flies, whole RNA was isolated from adults and analyzed in the same manner described above.

RNA interference: RNA interference (RNAi) was performed as described previously (Kennerdell and Carthew 1998). To synthesize the DNA template, forward (base pairs 62–79) and reverse (base pairs 908–893) primers flanking an 846-bp region of the *sda* sequence were made. Each primer had on the 5′ end a 30-bp sequence 5′-CGGATCCTAATACGACTCACTATAGGGAGA-3′, which contains a T7 promoter sequence (underlined) for *in vitro* transcription and extra nucleotides to optimize efficiency. The transcription was performed using the RNA transcription kit from Stratagene. The double-stranded RNA (dsRNA) product was purified, precipitated, and assayed using A_{260} as described (Kennerdell and Carthew 1998). The dsRNA was dissolved in TE buffer to the desired concentration and was injected into *w^{1118}* embryos (less than stage 3), using a needle with a tip opening of 0.5–2.5 μm. Injected embryos were covered with Halocarbon 600 oil and placed at 18° in a moist box for recovery. After hatching the surviving larvae were transferred to a culture vial, grown to adults at room temperature, and tested for BS behavior. For control experiments, separate collections of wild-type embryos were prepared and mock injected, injected with TE buffer, or injected with dsRNA (2.0 or 3.0 μM) prepared against the *sticky ch1* (*stich1*) coding sequence (Prokopenko *et al.* 2000).

Embryo and larval mRNA *in situ* hybridization: The experiments were conducted according to methods previously reported (Kopczynski *et al.* 1998). The DNA template used spans base pairs 62–908 of the *sda* LP11029 transcript. The antisense (reverse) primer has a T7 promoter sequence to synthesize specifically antisense *sda* RNA. RNA synthesis was performed using the GIBCO Riboprobe synthesis kit that uses digoxygenin-labeled uridine. The labeled antisense RNA molecules were hybridized to whole embryos, and color visualization was produced using anti-digoxygenin alkaline phosphatase-conjugated antibodies. The final stained embryos were mounted on slides and examined under a digital compound microscope. Photos were taken using the program Spot and

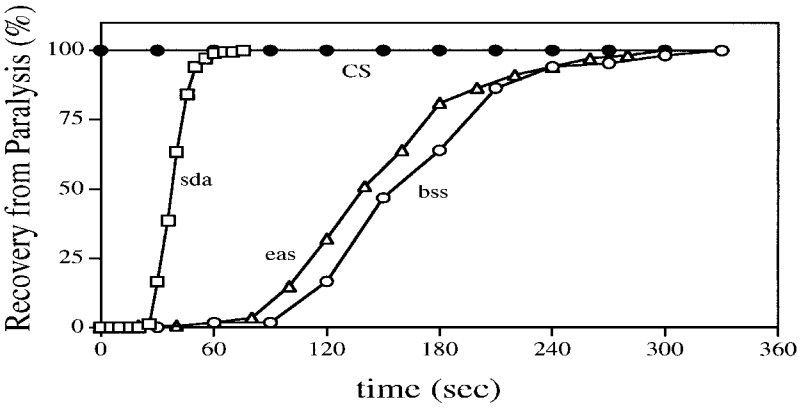

FIGURE 1.—Behavioral analysis of *sda* and other BS mutants. Flies of the genotype indicated were shocked mechanically in batches of 10 flies in an empty food vial on a vortex mixer (10 sec at maximum setting) and allowed to recover from paralysis. The number of flies standing at intervals following the shock was recorded until the entire population had recovered. A given population of flies recovers in a reproducible way, although there is tremendous variability in recovery times among the different genotypes. Shown are the percentage of flies recovered with time and a cumulative measure that includes the initial behavioral seizure, the paralysis period, and the recovery seizure, which are not indicated separately. Genotypes include CS (n = 100 flies), *sda* (n = 160 flies), *bss* (n = 100 flies), and *eas* (n = 149 flies).

prepared using Adobe Photoshop. For larval mRNA *in situ* hybridization, the third instar larval CNS was prepared using previously described methods (MASSUCI *et al.* 1990). Following CNS preparation, the rest of the experiment (probe synthesis, hybridization, and staining) was done as described for embryos.

LacZ reporter staining in $sda^{HZ.P1}$ adult CNS: Adults of $sda^{HZ.P1}$ were decapitated using forceps and the tissues immobilized by freezing in O.C.T. (Tissue-Tek). The frozen block was then sliced into 10-μm sections by cryostat, and the sections were blotted onto slides pretreated with poly L-lysine (Sigma, St. Louis). The tissues were fixed in 2% glutaraldehyde for 15 min and then washed three times in 1× PBS buffer for 5 min at room temperature. The slides were placed in staining solution with 1/30 volume X-Gal [composition of staining solution: 1.8 ml of 0.2 M Na_2HPO_4, 0.7 ml of 0.2 M NaH_2PO_4, 1.5 ml of 5.0 M NaCl, 50 μl of 1.0 M $MgCl_2$, 3.0 ml of 50 mM $K_3(Fe(CN)_6)$, and 3.0 ml of 50 mM K_4 $(Fe(CN)_6)$; total volume is brought to 50 ml with H_2O]. The sections were then stained until the desired intensity was obtained. Final results were photographed with a digital compound microscope and the pictures processed via Adobe Photoshop. A control experiment was performed with w^{1118} flies.

RESULTS

The *sda* behavior: The behavioral phenotypes of *sda* mutants are generally similar to other mutants of the BS paralytic class such as *bss*, *eas*, and *tko*. Undisturbed *sda* flies do not show notable defects in specific behaviors: They eat, walk, jump, fly, groom, court, and mate normally; they show usual positive-phototaxis and negative-geotaxis behaviors. There are no apparent alterations in the overall levels of activity such as hyperactivity or sluggishness. Behavioral abnormalities are induced in all homozygous *sda* mutants by a mechanical shock (a bang). The resulting behavioral phenotype is complex with five distinguishable phases: initial seizure, paralysis, recovery seizure, recovery with refractory period, and complete recovery. The initial behavioral seizure is characterized by leg shaking, abdominal muscle contractions, wing flapping, and proboscis extension; this phase usually lasts several seconds. This is followed by complete paralysis with no physical activity observed and distinguished by a relaxed state of the wings, legs, body, and proboscis; paralysis lasts ~20 sec. Each *sda* mutant then shows a postparalysis hyperactive phase or recovery seizure, characterized by massive uncoordinated motor activity somewhat similar to the initial seizure. Finally, the flies right themselves and resume normal behavior.

The recovery time (from the start of the bang to when the flies stand back up again) varies among different BS mutants (Figure 1). For example, in *sda* flies the time for 50% recovery is ~37 sec, faster than the recovery times for *eas* and *bss*, which are ~140 and 150 sec, respectively (Figure 1). All of the different BS strains are similar in initial seizure, paralysis, and recovery seizure. However, following the recovery seizure, only *sda* mutants recover immediately. Other strains, most notably *bss*, undergo additional bouts of paralysis and seizure that resemble tonic-clonic activity in human epilepsy and that can last for many minutes, thereby increasing the time of recovery. The relatively rapid recovery of *sda* mutants appears to be entirely due to the lack of any tonic-clonic activity. Following recovery, *sda* mutants resume normal behaviors. Interestingly, immediately following recovery, *sda* mutants cannot be reparalyzed by mechanical stimulation; that is, the mutants are no longer BS. This is termed "the refractory period" and is a transient period present in all BS genotypes, although it varies in duration among the different strains. For *sda* flies, the refractory period is ~7 min and is shorter than those for *eas* and *bss*, which are ~10 and 12 min, respectively.

The *sda* mutation is a weak semidominant in behavioral tests. Heterozygous *sda*/+ flies show mostly normal behavior, although a few (1–2%) are BS. The semidominant BS phenotype is more readily apparent if tests are performed exclusively on very young flies. For example, tests on young flies 1–2 days posteclosion show that as many as 45% can show some BS paralytic behavior. However, this phenomenon is not consistent across the other BS genotypes; for example, old *eas* and *bss* flies (>4 days) actually show a stronger paralytic phenotype

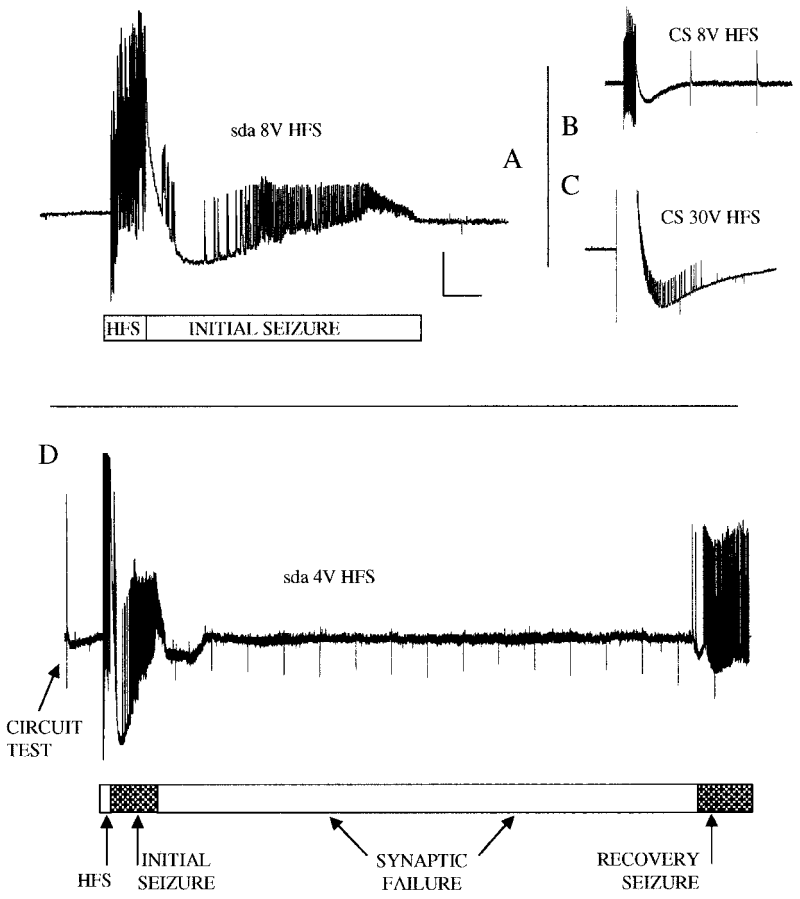

FIGURE 2.—Seizures in *sda* and CS flies. The mutant *sda* fly is more susceptible to seizures than the wild-type (CS) fly and therefore has a much lower seizure threshold. (A) A seizure is elicited in a *sda* fly by a high-frequency stimulus of low strength (8 V) and displayed at a high sweep speed. The HF stimulus (HFS) is a short wavetrain (0.5 msec pulses at 200 Hz for 300 msec) of electrical stimuli delivered to the brain. Recording is from a DLM muscle fiber and reflects the activity of the single DLM motoneuron that innervates it. The seizure is widespread as similar activity can be found in recordings from seven different muscle groups in the fly following HF stimulation (KUEBLER and TANOUYE 2000). (B) A low-voltage HF stimulus of 8 V fails to elicit a seizure in a wild-type CS fly because the stimulus is below the seizure threshold. Following the HF stimulus artifact, no seizure activity is observed in this recording displayed at a high sweep speed. Note also that there is no period of synaptic failure and single-pulse stimulation of the GF (0.5 Hz) continues to evoke DLM potentials. Two such effective single-pulse stimuli are depicted in this trace; each was effective in evoking a DLM potential. (C) A seizure is elicited in a wild-type CS fly by a high-voltage HF stimulus (30 V), which is above the threshold for seizure. The seizure in this recording begins within the large stimulus artifact and is displayed at a high sweep speed. (D) Same recording as for A from a *sda* fly, but displayed at a slower sweep speed. In this recording, the HF stimulus and seizure are followed by a quiescent period (SYNAPTIC FAILURE) that is characterized by synaptic failure within the GF circuit (PAVLIDIS and TANOUYE 1995). During this period, there are stimulus artifacts (downward-going) from continuous single-pulse stimulation of the GF (0.5 Hz), but no evoked DLM potentials. Spontaneous activity or "recovery seizure" appears as additional seizure-like activity occurring just after the synaptic failure period and just prior to recovery (recovery not evident in this trace). Vertical calibration bars are 20, 40, 40, and 10 mV for A, B, C, and D, respectively. Horizontal calibration bars are 300 msec, 1.2 sec, 1.2 sec, and 1.5 sec for A, B, C, and D, respectively (modified from KUEBLER and TANOUYE 2000, Figure 1).

than do young flies (1–2 days posteclosion; P. PAVLIDIS and M. TANOUYE, unpublished observations).

Seizure and failure in the GF pathway of *sda* adults: The electrophysiological phenotypes of *sda* mutants are generally similar to other mutants of the BS paralytic class such as *bss*, *eas*, and *tko*. In tests of the general properties of the GF system, *sda* flies responded normally. Stimulation of *sda* GFs with single stimulus pulses (0.5 msec, 0.8 Hz) produces DLM responses that are normal in appearance, threshold (2.2 ± 0.38 V), and latency (1.3 msec). When tested with twin pulses, *sda* DLMs followed GF stimuli separated by a minimum of 10 msec, similar to wild-type flies (TANOUYE and WYMAN 1980). When tested for following frequency by 20 stimulus pulses, *sda* DLMs followed at least 19 of the stimuli at a frequency of 131 ± 17.6 Hz, similar to wild-type flies (KUEBLER and TANOUYE 2000). Thus, under conditions of mild to moderate stimulation, the GF-DLM responses of *sda* are normal.

Electrophysiological analysis of *sda* mutants with HF stimuli shows that seizures may be induced in individual flies and that these mutants are particularly seizure sensitive compared to wild-type, similar to other mutants in the BS mutant class. We investigated the electrophysiological basis of *sda* seizure and paralysis using a standard protocol for stimulating and recording from the adult fly GF pathway that has been described previously (KUEBLER and TANOUYE 2000). The features of *sda* mutant electrophysiology described here are qualitatively similar to those reported previously for other fly genotypes (Figure 2A; PAVLIDIS *et al.* 1994; PAVLIDIS and TANOUYE 1995; KUEBLER and TANOUYE 2000; KUEBLER *et al.* 2001). "Seizures" in *sda* mutants following HF stimuli consist of aberrant high-frequency firing (>100 Hz) lasting for 2–3 sec and present in all the muscle fibers and motoneurons examined (KUEBLER and TANOUYE 2000). For *sda* males and females, seizure thresholds are 6.2 ± 0.8 and 6.8 ± 1.0 V, respectively. These seizure thresholds are considerably lower than those for male and female CS flies whose values are 30.1 ± 3.8 and 44.5 ± 4.4 V, respectively. Thus, using the criterium of HF stimulus threshold, *sda* mutants are five to seven times more seizure sensitive than wild-type flies. The next aspect of the phenotype is the sudden failure of

GF stimulation to evoke DLM potentials (Figure 2D). Such failure in the nervous system is due to synaptic failure in many central synapses and is likely the underlying cause of behavioral paralysis in *sda* mutants (Pavlidis and Tanouye 1995). The period of synaptic failure has been measured as 38.0 ± 7.0 sec in *sda* (Pavlidis and Tanouye 1995). Following the period of synaptic failure, a recovery seizure is observed that consists of aberrant high-frequency firing of the DLM motoneurons, similar to the initial seizure in scale and duration (Figure 2D).

The *sda* mutation is semidominant in HF electrophysiology. Heterozygous $sda^{iso7.8}$/+ mutants show a lower seizure threshold than do wild type (30.6 ± 4.5 V in heterozygous females *vs.* 44.5 ± 4.4 V in CS females). This is interesting to us as it suggests that, although appearing to be largely wild type in behavior and electrophysiology, *sda*/+ heterozygous mutants may be fairly close to expressing seizure-sensitive phenotypes. This suggests that heterozygotes could be used to provide a sensitized genetic background for detecting other mutations affecting seizure susceptibility such as weak BS alleles and BS enhancers.

Cloning and characterization of *sda*: We mapped *sda* to a small region on the third chromosome (97D1–5) defined by three closely spaced deletion breakpoints, *Df(3R)ro-XB3*, *Df(3R)ro-z1*, and *Df(3R)Bd* (Figure 3). Initial identification of the *sda* gene was made possible by the isolation of a lethal *P*-element allele, $sda^{HZ.P1}$ (Figure 3). Molecular access to the *sda* gene was via the $sda^{HZ.P1}$ mutation by the method of plasmid rescue of genomic DNA flanking the transposon insertion. Sequencing of the rescued genomic DNA fragment and comparison of the results with information available in the Drosophila database further confirmed a 97D location for the *sda* gene. Using the genomic fragment as a probe, we identified a genomic DNA clone from a λ-phage library; we sequenced this 8-kb fragment and used it to identify cDNA clone LP11029 from the Berkeley *Drosophila* Genome Project (Figure 4). Two transcripts are encoded by *sda*. One is a 4.8-kb transcript that corresponds to the full-length LP11029 cDNA. A second is a 2.2-kb transcript. Screening of multiple cDNA libraries has failed to identify a cDNA corresponding to the 2.2-kb transcript so its characterization is unavailable presently. Southern and Northern blot analysis of the LP11029 cDNA and 4.8-kb transcript shows that *sda* is a large gene that spans ~30 kb of genomic DNA and contains eight exons (Figure 3). Introns II and III are especially large intervening sequences of ~8 and 13 kb, respectively.

Sequence analysis of LP11029 revealed that it consists of 4811 nucleotides, 3213 of which code for a putative protein of 1071 amino acids. Comparison of the deduced protein with sequence databases revealed significant similarity to previously identified human APN (Figures 3 and 4; Look *et al.* 1989; Watt and Willard 1990; Yeager *et al.* 1992). The aminopeptidase encoded by *sda* is distinct from a recently described Drosophila sequence located at 84F6–85A3, which encodes for a dipeptidyl aminopeptidase that degrades the insect neuropeptide proctolin (Mazzocco *et al.* 2001). The deduced *sda* protein sequence displays canonical features present in human APN and other members of the M_1 family of zinc-dependent ectopeptidases. The sequence predicts an N-terminal cytoplasmic tail of 33 amino acids for *sda*. This cytoplasmic tail is longer than human APN due to the presence of 24 unconserved amino acids at the *sda* N terminus. The predicted *sda* protein contains a transmembrane segment of 25 amino acids and an ectodomain of 1013 amino acids. The gluzincin Zn^{2+}-binding motif [HEXXH-(18X)-E] that constitutes the core of the active site of both gluzincin aminopeptidases and endopeptidases is present in the *sda* protein, starting at amino acid position 486. In this segment of the protein, there is 84% identity between *sda* and human APN (26 identical residues out of 31 total amino acids in the segment). The GAMEN motif, identified as another conserved sequence motif in the gluzincin aminopeptidases, is present in the *sda* protein as AAMEN and is positioned 39 amino acids N-terminal to the Zn^{2+}-binding motif. In human APN, the conserved glutamate residue of this motif has been shown to be a crucial residue in an anionic binding site recognizing the free amino group at the N terminus of the substrate (Luciani *et al.* 1998). The overall amino acid similarity shows that the Drosophila protein is 33% identical and 51% similar to human APN and 31% identical and 50% similar to mouse APN. Substantially greater identity is observed in the catalytic portions of the ectodomain (Figure 4).

Molecular basis of *sda* mutations: We determined the molecular basis of the known *sda* alleles: the original isolate $sda^{iso7.8}$ and $sda^{HZ.P1}$ acquired in the course of this work. The exact insertion site of the *P* element of $sda^{HZ.P1}$ was found by sequencing the genomic DNA fragment from plasmid rescue using a primer targeting the end of the *P*-element sequence. This analysis showed that $sda^{HZ.P1}$ had inserted in exon I between nucleotides 61 and 62 in the 5′ untranslated region (UTR) of the gene. We determined the molecular basis for the spontaneous allele $sda^{iso7.8}$ by using RT-PCR to amplify the coding sequence of the *sda* gene in wild-type and mutant flies. The resulting products were sequenced and compared. This analysis revealed a 2-bp insertion in exon III between nucleotides 671 and 672 in the 5′ UTR of the gene (Figure 5). The molecular basis of both of the *sda* alleles is consistent with the LP11029 cDNA we identified as representing the *sda* gene. These results suggest that *sda* mutant phenotypes most likely arise from underexpression or perhaps misexpression of Drosophila APN.

RNAi of Drosophila APN causes BS phenotypes: We attempted to generate *sda* phenotypes in non-BS flies by altering normal levels of APN expression using the method of RNAi (Carthew 2001). RNAi was performed

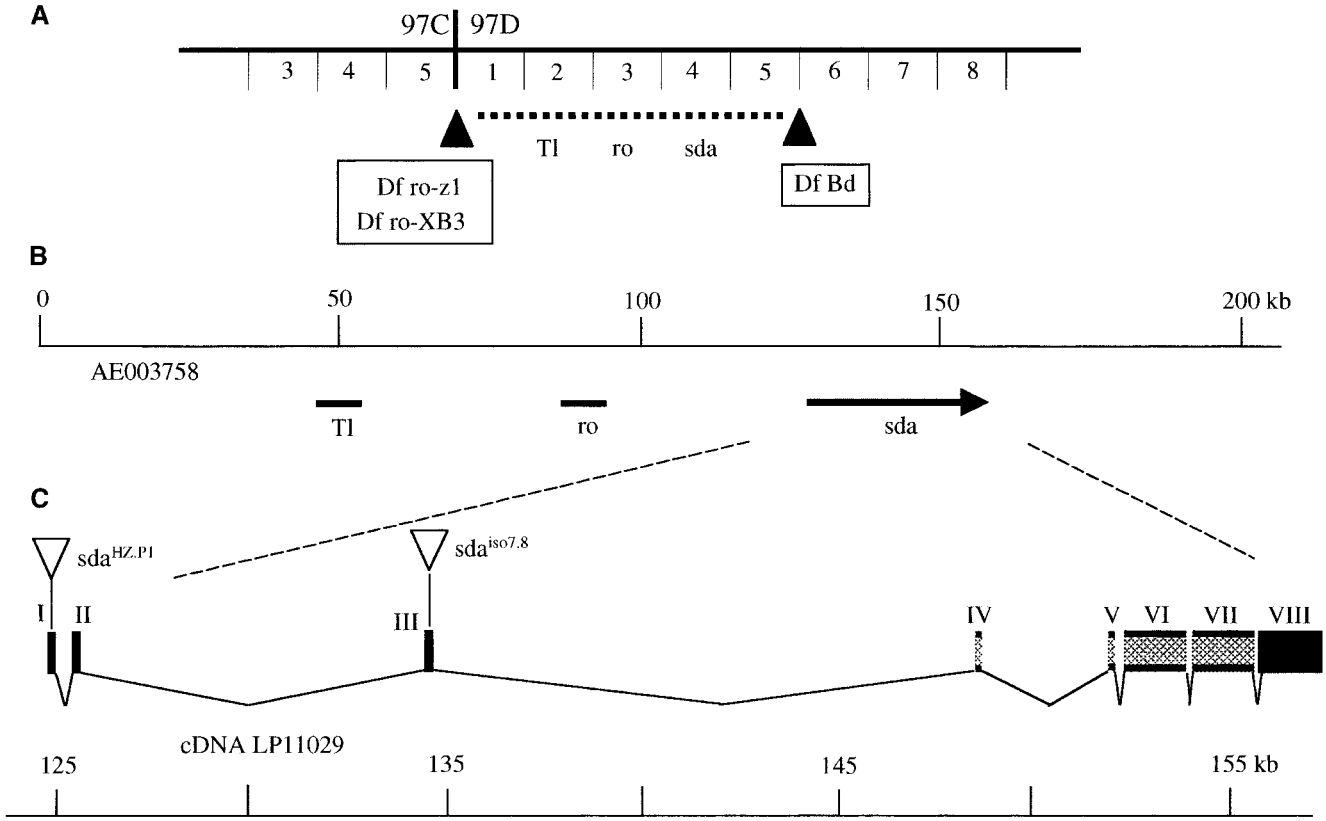

FIGURE 3.—Genetic and molecular representation of the 97D region that contains *sda*. (A) Cytogenetic analysis places the *sda* locus in a five-band region on the basis of its inclusion in *Df(3R)ro-xB3 = Df(3R)97D1-2; 97D9* and *Df(3R)ro-z1 = Df(3R)97D1-2; 97D15* and its exclusion from *Df(3R)Bd = Df(3R)< 97D5; 97F1-98A1*. The *sda* gene is located on the same scaffold as *Tl* (cytogenetic location 97D1–2) and *ro* (97D2–3) and maps to the right of both. Depicted is the 97D1–97D5 interval, the approximate locations of the defining deletion breakpoints marked with solid triangles, and the apparent order of *Tl ro sda* within the interval. (B) Depicted is a representation of scaffold AE003758 (Berkeley *Drosophila* Genome Project), showing ~200 kb and the relative locations of the *Tl, ro*, and *sda* genes. Arrow for *sda* indicates the direction of transcription. (C) A blowup showing the genomic organization of the full-length cDNA LP11029. Roman numerals designate exons. The stippled bars within the cDNA represent coding sequences. Small open triangles indicate the location of the $sda^{HZ.P1}$ *P*-element transposon insertion in exon I and the $sda^{iso7.8}$ insertion in exon III; both insertions are located in the 5′ UTR.

using dsRNA corresponding to an 824-bp segment of the *sda* coding transcript. We injected w^{1118} embryos with a 1.8-μM solution of dsRNA and assayed for BS behavior among the surviving adults. Results from the experiment showed that 31 of the 34 surviving adults exhibited a BS behavioral phenotype: They became paralyzed following mechanical stimulation. The BS behavioral phenotype persisted in these flies for at least 10 days. There were some quantitative differences between the RNAi-treated flies compared to $sda^{iso7.8}$ mutants. The recovery time was shorter for the RNAi-treated flies (15 sec) compared to the mutant (37 sec); also, the refractory period was shorter for the RNAi-treated flies (3 min) compared to the mutant (7 min). Control injections using non-APN dsRNA (2.0 or 3.0 μM) yielded flies with no discernible BS phenotype. The indication from this analysis is that specific alteration of APN expression by RNAi is sufficient to generate BS behavioral phenotypes in wild-type animals. We also tried a lower concentration of APN dsRNA (0.9 μM). Surviving adults (30 flies tested) did not become paralyzed by the mechanical stimulus, but many of them showed an unusual neurological defect of "wobbliness" manifest as unsteady legs and shaky movement. This type of phenotype has not previously been associated with BS mutants, but has been observed in other BS genetic combinations in our collection (D. HEKMAT-SCAFE and M. TANOUYE, unpublished observations). These results suggest that the BS phenotype observed in $sda^{iso7.8}$ mutants is the consequence of the lesion found in the *sda* gene, for two reasons: (1) When we inhibit the expression of the gene in non-BS flies by introducing dsRNA, we can mimic the BS phenotype observed in *sda* mutants, suggesting that the gene product is directly related to bang sensitivity, and (2) the fact that interference appears to be proportional to the concentration of dsRNA used implies that the observation is a true representation of gene interference and not just a coincidence.

***sda* mRNA: Northern blot analysis:** From our results of the RNAi experiment and analysis of the nature of

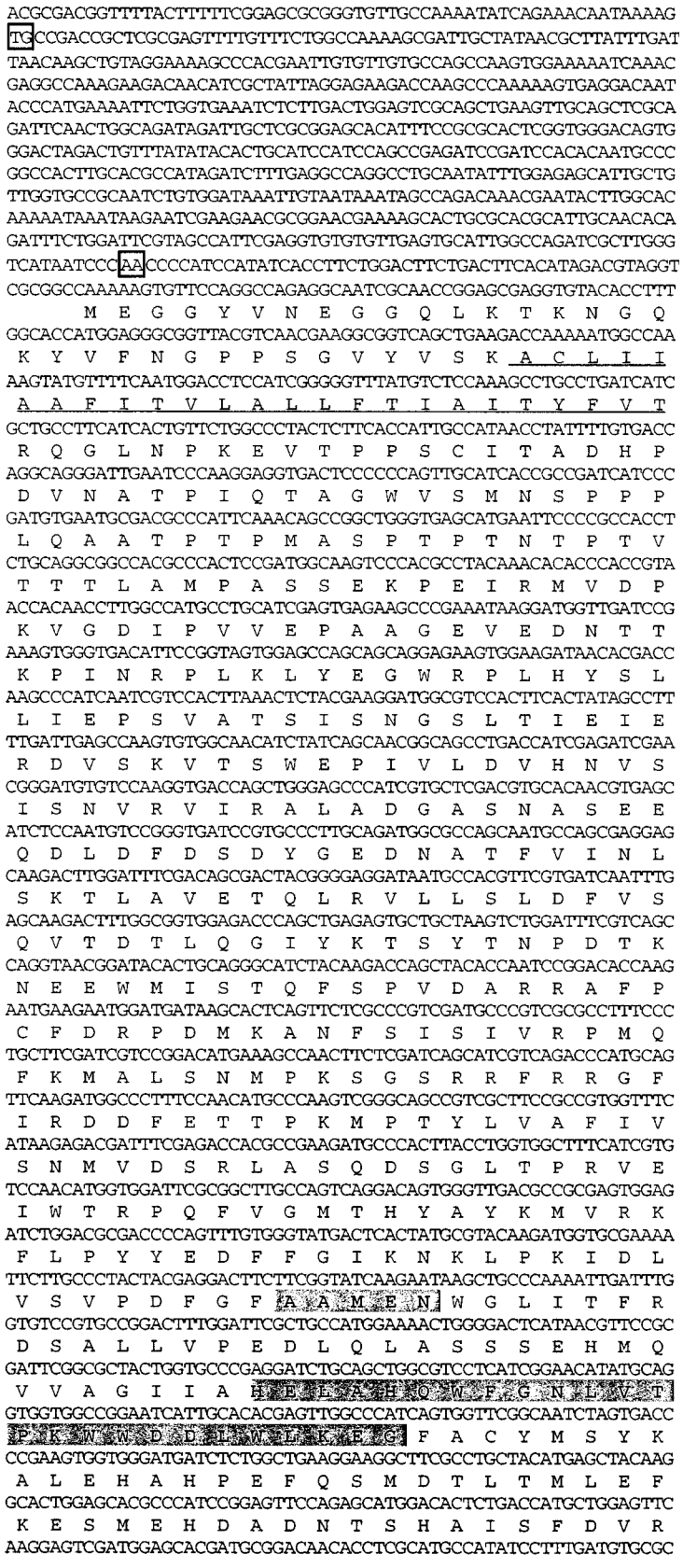

FIGURE 4.—Sequence of a *sda* cDNA. Shown is the complete sequence of cDNA clone LP 11029 with its predicted amino acid translation product. The insertion site of the $sda^{HZ.P1}$ *P*-element transposon between nucleotides 61 and 62 is indicated by a box, as is the insertion site of $sda^{iso7.8}$ between nucleotides 671 and 672. The predicted membrane-spanning segment is indicated by the underline from amino acid position 34 to 58. Shading indicates the glucinzin Zn^{2+}-binding motif [HEXXH-(18X)-E] beginning at amino acid position 486 and the GAMEN motif (AAMEN in the *sda* sequence) beginning at amino acid position 447.

molecular lesion in the *sda* mutants, it appears that the molecular defect associated with the *sda* mutation is very likely an abolition or at least a downregulation of *sda* gene expression. To test our hypothesis, we performed a Northern blot comparing *sda* gene expression between wild-type and $sda^{iso7.8}$ adults (Figure 6). The results dem-

```
 559   S  T  N  D  V  R  R  I  F  D  P  I  S  Y  S  K  G  T  I  L
2461  TCCACCAACGATGTCAGGCGGATTTTCGATCCCATCAGCTACTCAAAGGGCACCATTCTG
 579   L  R  M  L  N  S  I  V  G  D  V  A  F  R  S  A  T  R  D  L
2521  CTGCGCATGCTCAATTCGATCGTGGGTGATGTGGCCTTCCGGTCGGCCACTCGTGATCTT
 599   L  K  K  F  A  Y  G  N  M  D  R  D  D  L  W  A  M  L  T  R
2581  CTAAAGAAGTTCGCCTATGGAAACATGGACAGAGATGATCTGTGGGCCATGCTCACGCGC
 619   H  G  H  E  Q  G  T  L  P  K  D  L  S  V  K  Q  I  M  D  S
2641  CATGGTCACGAACAGGGTACTCTGCCCAAGGATCTGAGTGTCAAGCAGATCATGGACTCG
 639   W  I  T  Q  P  G  Y  P  V  V  N  V  E  R  R  G  A  D  L  V
2701  TGGATCACCCAGCCCGGTTATCCGGTAGTCAATGTGGAGCGCCGTGGTGCTGATCTCGTG
 659   L  R  Q  E  R  Y  L  L  P  S  K  N  T  A  D  Q  S  T  W  F
2761  CTGCGCCAGGAACGCTATCTGCTGCCCTCCAAGAACACTGCGGATCAGAGCACCTGGTTT
 679   I  P  I  T  F  E  T  D  E  L  R  K  G  D  N  I  P  T  H  W
2821  ATACCCATCACCTTCGAGACGGATGAGTTGCGCAAGGGCGACAACATACCCACCCACTGG
 699   M  R  S  E  D  E  E  E  L  I  V  G  N  V  F  A  H  S  S  N
2881  ATGAGAAGCGAGGACGAAGAGGAGCTCATCGTGGGCAATGTCTTCGCGCATAGCAGCAAC
 719   S  D  N  V  I  Y  L  N  L  N  R  Q  G  Y  Y  R  V  N  Y  D
2941  AGCGATAACGTGATCTATCTGAATCTCAACCGGCAGGGTTACTATCGTGTCAACTACGAT
 739   M  T  S  W  L  A  L  K  K  N  F  S  T  L  P  R  I  T  R  A
3001  ATGACCTCTTGGCTGGCGCTCAAGAAGAACTTTAGCACATTGCCCAGGATCACAAGGGCC
 759   Q  L  L  D  D  A  L  H  L  S  Q  A  E  Y  L  T  Y  D  I  P
3061  CAGTTGCTGGATGATGCACTGCATCTGTCGCAAGCGGAATACCTTACCTACGACATACCA
 779   L  T  F  L  M  E  L  F  D  A  V  D  D  E  L  L  W  I  A  A
3121  TTGACCTTCCTCATGGAGCTGTTCGATGCTGTGGATGATGAGCTGCTGTGGATTGCCGCC
 799   K  P  G  L  N  Y  L  I  Y  N  L  K  R  E  P  A  Y  E  T  F
3181  AAACCTGGTCTCAACTATCTGATCTACAACCTGAAGAGGGAGCCTGCCTATGAGACTTTC
 819   R  A  F  M  K  F  I  V  R  P  A  F  D  H  Y  G  L  H  E  P
3241  AGGGCCTTCATGAAATTCATCGTACGTCCCGCCTTTGATCATTATGGCCTGCATGAGCCG
 839   D  N  E  S  H  L  Q  L  K  H  R  A  L  V  A  Y  F  A  C  K
3301  GACAATGAGTCCCACTTGCAACTGAAGCACCGCGCCTTGGTGGCCTACTTTGCCTGCAAG
 859   F  N  Y  D  R  C  T  Q  K  A  Q  M  K  F  R  E  W  M  R  D
3361  TTCAACTACGATCGCTGCACCCAAAAGGCGCAGATGAAGTTCCGCGAGTGGATGCGTGAT
 879   P  K  N  N  P  I  K  P  N  L  K  S  V  I  Y  C  T  S  L  A
3421  CCCAAAAACAATCCCATTAAGCCAAACCTCAAGTCTGTGATCTACTGCACCTCCTTGGCG
 899   E  G  S  S  P  E  W  Y  F  A  Y  K  Q  Y  K  T  T  T  S  A
3481  GAGGGCTCGTCACCGGAATGGTATTTCGCCTACAAACAGTACAAGACAACCACGAGTGCT
 919   S  E  K  E  E  I  L  T  S  L  G  C  T  T  K  P  W  L  L  S
3541  TCCGAGAAGGAGGAGATACTGACCTCACTGGGCTGCACCACCAAACCCTGGCTGCTGTCC
 939   K  Y  L  N  M  T  I  N  P  T  S  G  I  L  K  Q  D  G  A  L
3601  AAGTACCTCAACATGACCATCAATCCAACATCGGGCATACTAAAACAGGATGGCGCCTTG
 959   A  F  R  A  V  A  S  N  A  I  G  H  E  I  A  F  D  F  L  Q
3661  GCCTTCCGTGCTGTGGCCTCCAATGCCATTGGTCATGAGATAGCCTTTGATTTTCTGCAG
 979   G  N  I  K  E  I  V  E  Y  Y  G  D  G  F  S  T  L  S  E  M
3721  GGCAACATAAAGGAGATTGTCGAATACTATGGCGATGGCTTCTCCACGCTGTCCGAGATG
 999   I  K  S  L  T  I  Y  M  N  K  D  Y  H  K  H  Q  L  L  D  L
3781  ATCAAATCGCTGACCATCTACATGAACAAGGACTACCATAAGCACCAGCTTCTGGACTTG
1019   A  A  T  C  R  K  L  G  L  H  A  V  E  S  A  I  E  L  A  L
3841  GCCGCTACCTGCCGCAAACTGGGACTCCATGCCGTGGAATCGGCCATCGAGTTGGCGCTG
1039   E  Q  V  N  N  N  I  Y  W  R  S  H  S  Y  H  S  L  K  N  F
3901  GAGCAGGTGAACAACAACATCTATTGGCGCAGCCACTCGTACCACAGCCTGAAGAACTTC
1059   L  E  G  I  V  S  E  F  Q  I  N  I  F
3961  CTTGAGGGGATCGTCAGCGAGTTCCAGATCAATATCTTTTAGGAGAACACATGGAAGTTG
4021  GAAATGGGGGAGAACTCAAATTGATTTCAACCAAAAAATGCGATTTAGTTATTGTAACTA
4081  TTACCATTATTTGTATTCGTGCAAAGGCCTCAAATTAATTTAATCAAACGAATTATTTGC
4141  GAAAAGTGATATAAACGTGTAAGTTAGCCAGCATAATTTAGGTAAACGATTTACTTTTTG
4201  CAATTGTATATTTATTTATTTGTAAGTCTCGCTTCTTTTGCTTTGCGGCATTGCTCTGCA
4261  ACGTTCCTACTAAAAAATAGAAAGCAATCGGAAAATGCATAGTTCGAATAACTCCCATTC
4321  ATCACTTCAGGCAACAGTTTAAGTCCACAACACAATATCTGCCACGAAATATCTAAAGTT
4381  TAAAACCTGTATTATCTATATCTATATCTATACTTATGATTGTCAAGTACTTTGTGTTGT
4441  TCGCACACCTTTAGATCCTAAGTGAATCAATCTAGCACTAAGTGAACCAAAAATCTATTT
4501  TGTAGTCGATCCAATCAAGGGACTTAATGGTCCTGGAAGGAAACTGAGCATGGGAAGATA
4561  ATGAAACTGAGTGTCCTTAGTACATGGTTTAAATTGTTTGCTAAAGCAAGAGTAGTACAC
4621  AACACACAACACACAAGTAATATATTTATTCATGTACGCGTGTAACTATTATGTATTTTG
4681  TAAAGCCCAACACAAAAATACTTGTATTGCTGCTGCACAACCATGTAAATAAGTTTTAAA
4741  GCTTACACTAAACACTTAAATAAACTATGTATTTACGTAAAAAAAAAAAAAAAAAAAAAA
4801  AAACTCGAG
```

Figure 4.—*Continued.*

onstrate that while the 2.2-kb variant is expressed at low levels in both wild-type and mutant flies, the 4.8-kb variant is present only in the former but not the latter. This observation supports our RNAi results and provides a further link between the *sda* gene and the BS phenotype.

We also performed a developmental Northern blot of wild-type flies (embryos, third instar larvae, and adults; data not shown) to characterize the temporal expression of the gene. Our results show that the 4.8-kb *sda* transcript is expressed throughout development, with expression highest in the adult stage and lowest in the

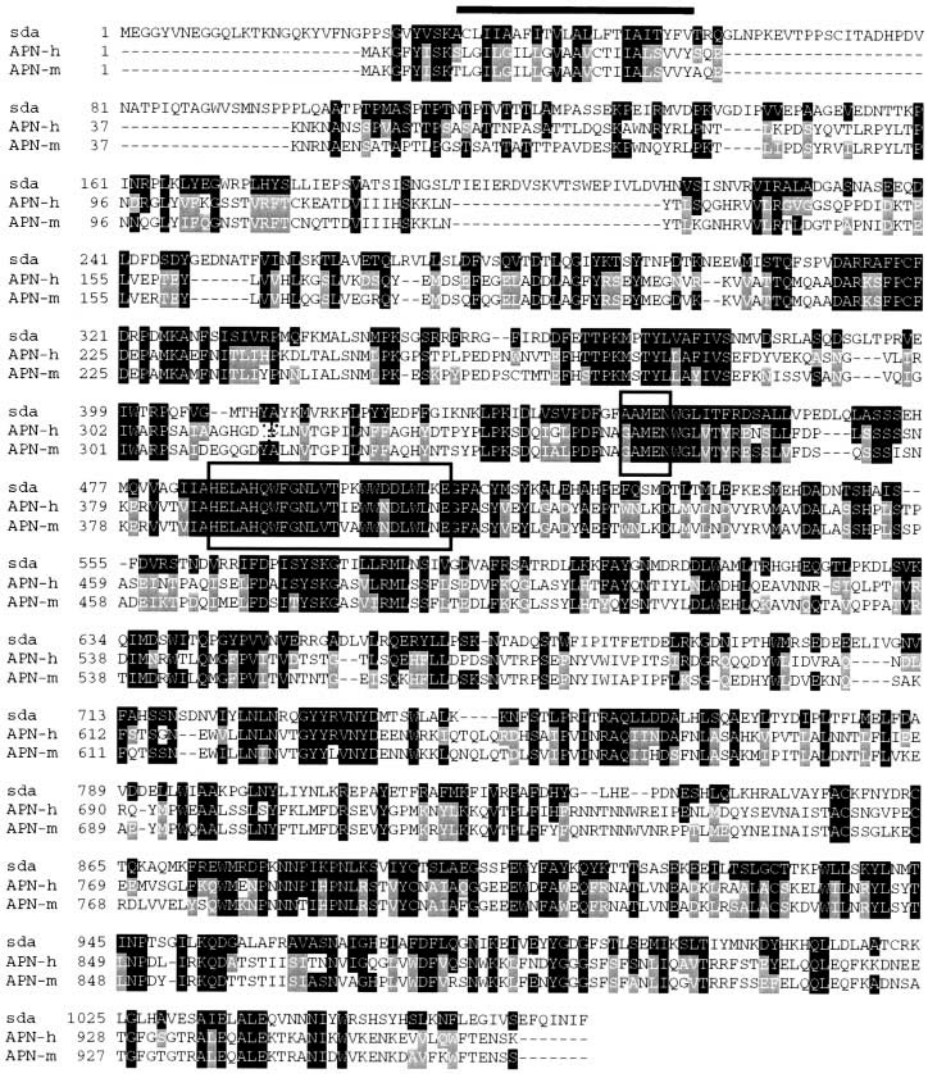

FIGURE 5.—Sequence homology of the predicted *sda* gene product. Sequence homology of the predicted *sda* protein product with human APN (APN-h) and mouse APN (APN-m) members of the M_1 family of zinc-dependent metallopeptidases (OLSEN *et al.* 1988; STRAUSBERG 2001). Amino acid identities are indicated by solid boxes and similarities are indicated by shaded boxes. Overall, *sda* is 33% identical and 51% similar to human APN and 31% identical and 50% similar to mouse APN. The thick solid bar indicates the predicted membrane-spanning segment of *sda*. Open boxes indicate the glucinzin Zn^{2+}-binding motif [HEXXH-(18X)-E] and the GAMEN motif (AAMEN in the *sda* sequence).

embryonic stage; the 2.2-kb transcript is also expressed in each of the three stages examined, although the expression pattern differs notably from that of the longer splice form. For the 2.2-kb transcipt, expression is lowest in the adult and highest in third instar larva. In all three stages examined, expression of the 4.8-kb transcript is greater than that of the 2.2-kb variant.

mRNA *in situ* and LacZ reporter analysis: To better understand how *sda* might function in the organism, we examined its gene expression at various developmental stages using mRNA *in situ* hybridization and LacZ reporter staining. In our embryo *in situ* experiment, we found that *sda* is initially expressed at very low levels (stages 1–12), but starting at stage 13 its expression drastically increases (Figure 7). During stages 13 and 14, *sda* is expressed profusely in the spiracle region, proventriculus, and, most interestingly, in distinct patterns in the CNS. This pattern changes from stage 15 onward as expression in the CNS and spiracle regions decreases (but is still notable) while expression in the proventriculus and gut regions increases (Figure 8). We compared the expression pattern of *sda* between wild-type flies and *sda* mutants and found no gross differences in terms of the locality in which *sda* is expressed or the intensity of its expression (Figures 6 and 7).

Since *sda* expression is observed in embryonic CNS, we were curious to see if it is expressed in the CNS of later stages. Therefore, we performed a mRNA *in situ* hybridization specifically on excised CNS from third instar larvae (Figure 8). We found, to our curiosity, that *sda* is expressed prominently in the ventral ganglion in three small but distinct clusters. Although at present we do not know for certain what these clusters represent, it is likely that they are groups of neural precursors.

And finally, since the *sda* BS phenotype is an adult phenomenon, we sought to analyze the gene expression in the adult CNS. To achieve this we sectioned heads of $sda^{HZ.P1}$ flies and utilized the LacZ reporter gene located in the *P* element as a reporter to see how *sda* is expressed in the CNS. The results we obtained are shown in Figure 9. There is prominent staining in the mushroom bodies, protocerebrum, and antennae (although the exact identity of the cells stained is not known), and the results are very consistent when com-

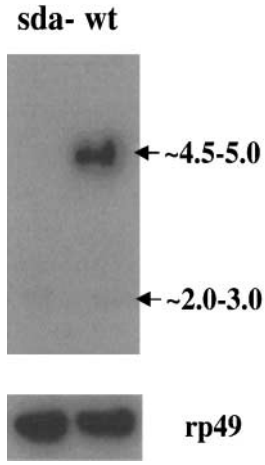

FIGURE 6.—Northern blotting of wild-type *vs. sda* adults. Whole RNA was extracted from both wild-type (wt) and *sda* mutant (sda−) adults, run on a denaturing gel, blotted onto nitrocellulose membrane, and probed with a fragment specific for the 5′ UTR of the *sda* CDS. The results indicate that the 4.8-kb transcript of the *sda* gene (LP11029) is expressed only in wild-type adults but not in mutant adults. A second variant (~2.2 kb) also appears to be expressed in both mutant and wild-type flies, but its constituency and identity are currently unknown (see text). We also probed for ribosomal protein 49 (rp49) to ensure that equal amounts of RNA were loaded for both wild-type and *sda* strains.

pared across similar sections. Rough estimates suggest that 40–50 cells in the protocerebrum, 20–30 cells in the mushroom bodies, and 30–40 cells in the antennae express *sda*. Control experiments performed with w^{1118} adults showed no discernible staining and eliminate the possibility that the staining from $sda^{HZ.P1}$ heads arises from endogenous β-galactosidase activity.

***sda* enhancer screen:** We examined the possibility that $sda^{iso7.8}$/+ heterozygotes could provide a sensitized genetic background, facilitating the identification of new BS paralytic mutants. An interesting feature of the BS mutant class is that each of the mutants thus far examined has been extremely seizure sensitive. The characterization of new BS mutations in Drosophila could improve our understanding of factors influencing seizures and give new insight into the difficult problem of human seizure disorders. As shown, the $sda^{iso7.8}$ mutation acts as a semidominant allele in electrophysiology and behavioral tests. Thus, we hypothesized that $sda^{iso7.8}$/+ could provide a background for detecting new mutations affecting seizure sensitivity. *P* elements were used as a mutagen and mobilized in dysgenic attached-X females; female progeny from this mobilization were then crossed with $sda^{iso7.8}$ males. The offspring were tested by mechanical stimulation, selecting for those displaying behavioral paralysis.

The resulting progeny are doubly heterozygous for $sda^{iso7.8}$ and the transposon insertion. We examined 12,000 chromosomes and isolated 15 mutant lines (Table 1). These doubly heterozygous lines varied in the percentage of flies susceptible to seizures. For example, line M showed the weakest phenotype with 40% paralysis for the double heterozygotes (genotype M +/+ $sda^{iso7.8}$). Apparently, the transposon of M acts as a weak dominant

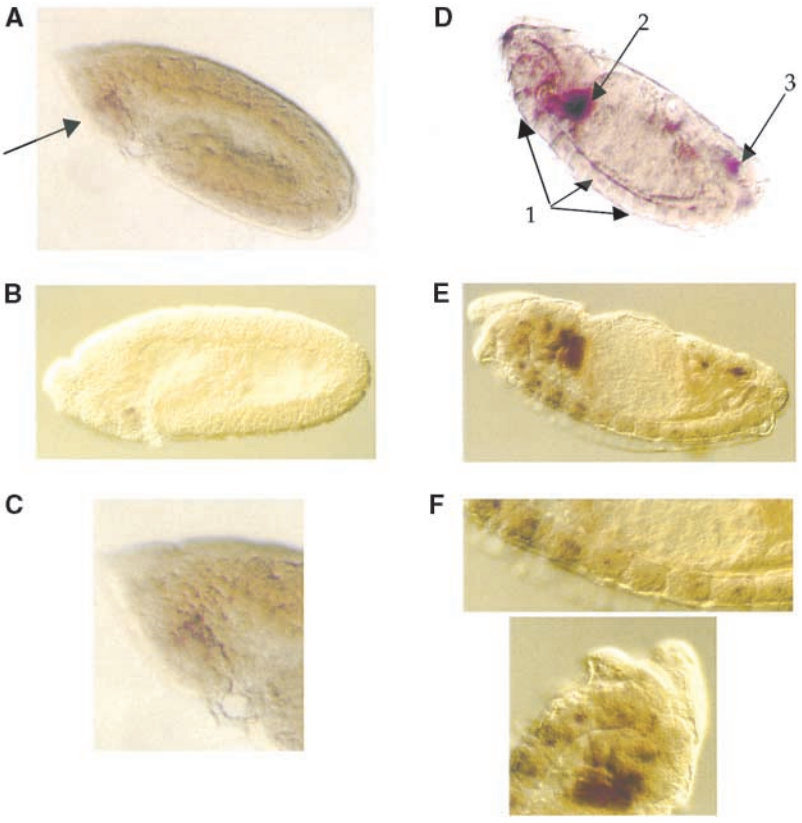

FIGURE 7.—Expression of *sda* in early and middle embryonic stages. The expression of *sda* in the embryonic stages may be categorized into three phases: early stage (stages 1–11), middle stage (stages 12–14), and late stage (stages 15–17, shown in Figure 8). Expression was probed using mRNA *in situ* with an antisense RNA probe specific to the *sda* gene. (A–C) The early-stage expression for wild-type embryos, *sda* mutant embryos, and a blowup of the stained area in wild-type embryos, respectively. Here we observed very little expression of *sda*, with only a barely notable staining in the putative CNS region. (D–F) The middle-stage expression pattern for wild-type embryos, *sda* mutant embryos, and a blowup of regions of prominent expression from the wild-type picture, respectively. During this period *sda* is expressed profusely in the CNS (arrow 1), putative gut (arrow 2), and the spiracles (arrow 3). Note in particular the expression in the CNS. Taking into account possible discrepancies due to experimental preparations and photographic techniques, we cannot discern any gross differences between wild-type and *sda* mutant embryos in the locality or intensity of *sda* expression.

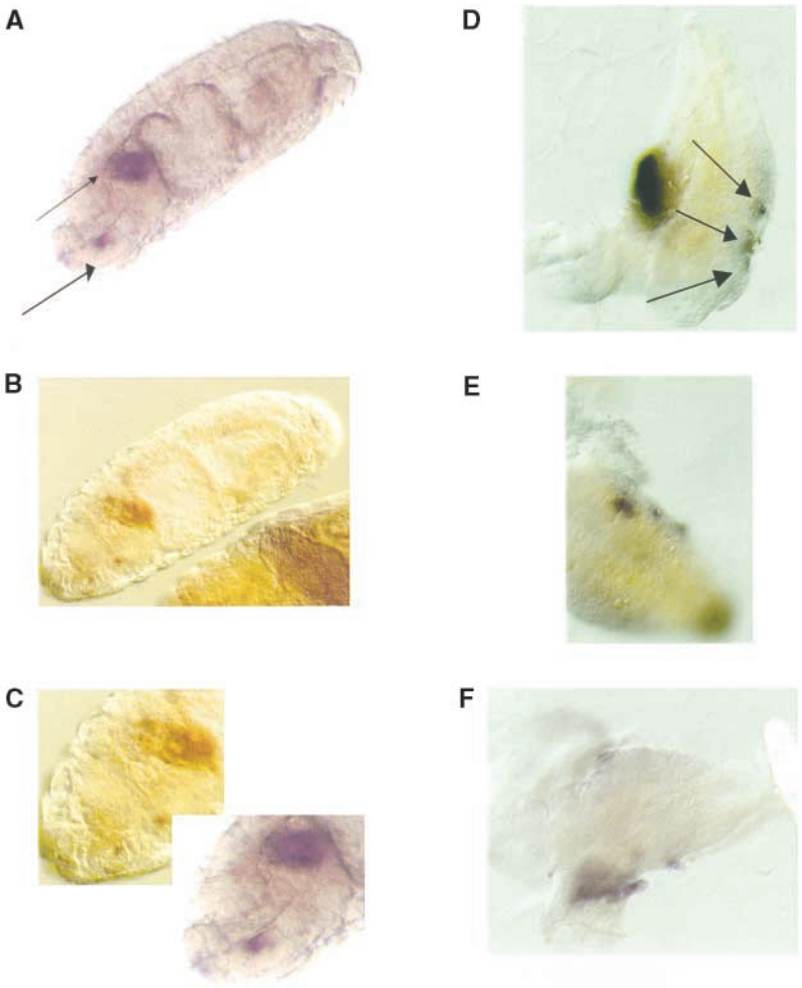

FIGURE 8.—Expression of *sda* in late embryonic stages and in the larval CNS. Expression was probed using mRNA *in situ* with an antisense RNA probe specific to the *sda* gene. The larval CNS was dissected from third instar larvae and stained as for embryos; only the ventral ganglion is shown since staining is restricted to this region of the CNS. (A–C) The late-stage expression for wild-type embryos, *sda* mutant embryos, and a blowup comparison, respectively. During this interval *sda* expression seems to be reduced compared to the middle stage, especially in the CNS and the spiracle region; in the putative gut, however, expression remains very strong. When compared to each other, again we do not see any gross discrepancies in *sda* expression between wild-type and mutant embryos. (D–F) The expression of *sda* in the wild-type larval CNS. Interestingly, here we see that *sda* is expressed in three tiny clusters bilaterally symmetric on the surface of the ventral ganglion. Although we do not know currently what they are, they are very likely neuronal precursors to certain subclasses of neurons. This three-cluster staining is observed in all the larval CNS dissected and stained ($n = 12$) and must be distinguished from nonspecific staining that occurs randomly and occasionally among the specimens.

enhancer of the antimorphic nature of $sda^{iso7.8}$. Line A showed a stronger phenotype with 100% paralysis for the double heterozygotes (genotype A +/+ $sda^{iso7.8}$). Apparently, the transposon of A acts as a strong dominant enhancer of the antimorphic character of $sda^{iso7.8}$.

For each of the isolated lines, we performed the appropriate crosses to remove $sda^{iso7.8}$ from the background and homozygose the transposon. Five lines (lines A, D, F, J, and O; Table 1) each had flies that paralyzed following mechanical stimulation (10–100%), suggesting that their respective *P* elements may have identified new members of the BS paralytic class. Four lines (lines G, H, I, and N; Table 1) yielded no homozygous mutant progeny, suggesting that the transposon caused a recessive lethal mutation. For four other lines (lines B, C, L, and M; Table 1) viable, homozygous mutant flies displayed no discernible phenotypes; the mechanisms by which these act to enhance the *sda*/+ phenotype remain unclear. *P* elements were mapped to various second and third chromosome locations by chromosomal *in situ* hybridization as indicated in Table 1. For each line, genomic DNA was isolated by plasmid rescue. DNA sequence analysis has identified several gene candidates, including a filamin actin-binding protein gene at 59A (line D), a helix-loop-helix protein gene at 86B (line A), and an RNA-binding protein gene at 90D (line N).

DISCUSSION

The *sda* gene encodes a Drosophila APN: Molecular mapping has localized the Drosophila *sda* mutations $sda^{iso7.8}$ and $sda^{HZ.P1}$ to a transcription unit that displays similarity to the human APN gene. RNAi analysis has shown that interference with Drosophila APN expression in wild-type animals causes behavioral abnormalities that resemble those observed in $sda^{iso7.8}$ mutants. These observations taken together strongly suggest that *sda* is Drosophila APN and that defects in its normal gene function are responsible for all of the observed mutant phenotypes, including a lowered threshold to seizures induced by HF stimuli. This role of altered excitabilities in the nervous system has not been suggested previously and adds to the extensive list of functions that are known for human and mouse APN.

The nature of *sda* mutations: Molecular examination of $sda^{iso7.8}$ and $sda^{HZ.P1}$ indicates their molecular lesions as a small deletion and insertion into the 5′ UTR of *sda*, respectively. Our expectation is that both mutations

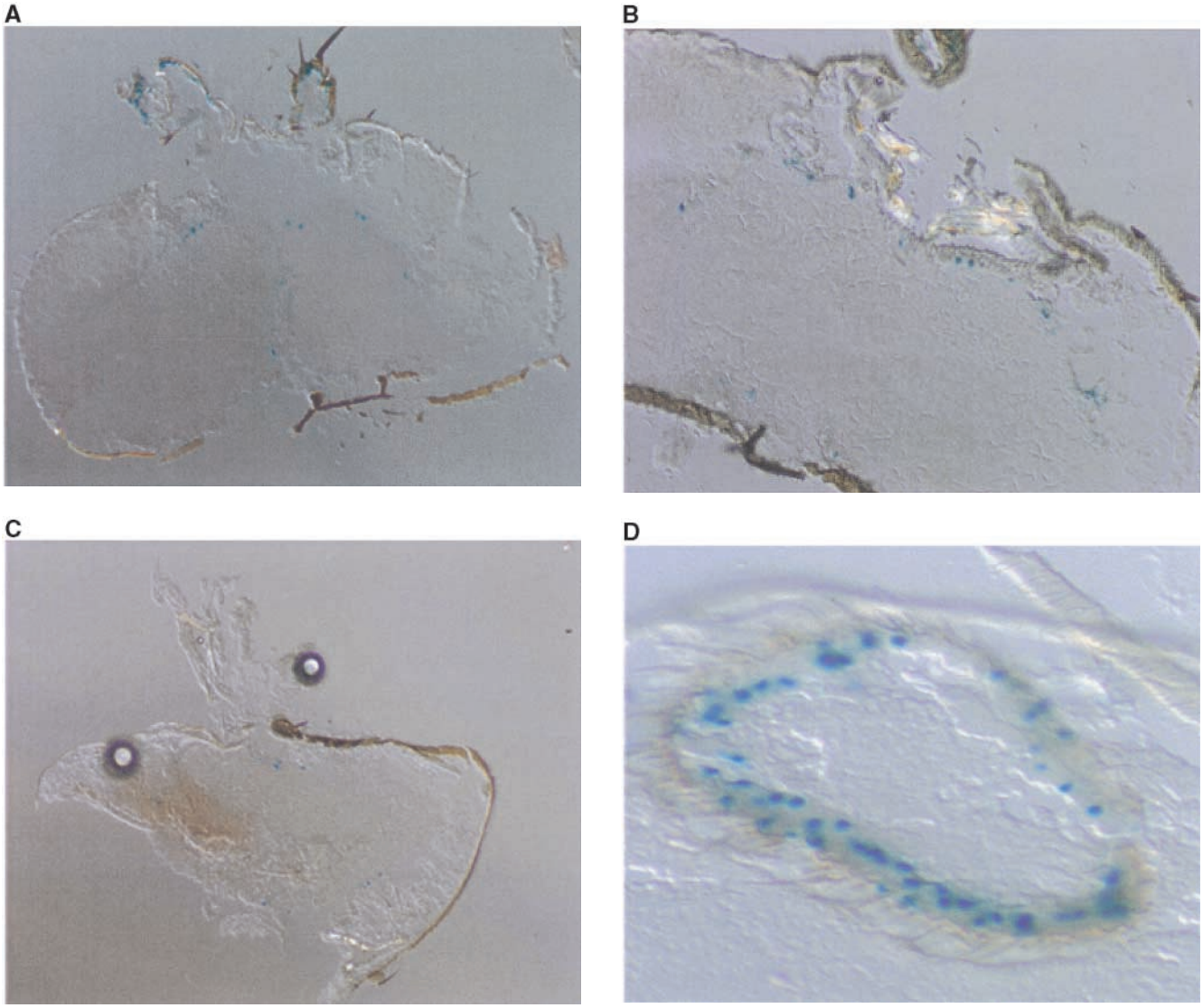

Figure 9.—LacZ reporter staining in adult CNS. $sda^{HZ.P1}$ adults were decapitated, their heads placed in an embedding medium, and the tissues immobilized by freezing. The heads were then sliced into 10-μm sections and mounted on pretreated slides. (A–C) Various sections of the head; note the peculiar semicircular nature of *sda* expression in the CNS, which is located in the mushroom bodies and protocerebrum. Finally, D shows an antenna with substantial staining in the areas directly beneath the cuticles. Blue spots denote the region of observed LacZ staining.

should cause alterations in *sda* expression in the form of downregulation or misexpression. The former possibility would fit in well with the RNAi results leading to BS phenotypes. This idea is indeed strongly supported by our Northern blot analysis comparing *sda* expression of wild-type *vs.* $sda^{iso7.8}$ mutant adults (Figure 6). It is interesting to note here, however, that our embryo mRNA *in situ* results do not demonstrate any gross differences in expression of *sda* between the wild-type and mutant strains. There are several possible explanations for this. The simplest reason could just be that *sda* expression (the 4.8-kb variant) in mutants is not downregulated until a later stage. A second possibility might be that the staining performed in the *in situ* hybridization was indiscriminate between the 4.8- and the 2.2-kb splice variants (since the probe spans the 5′ UTR, a region that appears to be shared by both variants) so that the results cannot distinguish the absence of one or the other; as a result, staining might appear similar although one variant may be entirely absent. Nonetheless, the fact that *sda* is not expressed in mutant adults is very strong evidence for the gene being responsible for the BS phenotype and also is consistent with our RNAi data. We are currently trying to raise antibodies to the SDA protein to conduct antibody-staining experiments to further document the localization of the *sda* gene product as well as fine-tune our mRNA *in situ* results.

A role for APN in nervous system excitability: There are several possibilities for how APN might alter nervous system function or structure and thereby contribute to

TABLE 1

Enhancer of *sda* mutations

Line	Paralysis *sda*/+ (%)	Paralysis BS (%)	Description	*P* site	Candidate gene
A	100	100	BS	86B	Helix-loop-helix protein; insertion is 80 bp upstream of gene
B	47	0	Enhancer	85D	Transketolase; insertion in promoter of gene
C	46	0	Enhancer	51F9	DNA mismatch repair protein; insertion is 1.7 kb upstream of promoter
D	66	84	BS	59A	Filamin actin-binding protein; insertion in third intron of gene
F	93	33	BS	47F	Translocation protein; insertion in or near putative exon region
G	53	Lethal	Enhancer	89B	Glycoprotein; insertion in first intron of gene
H	75	Lethal	Enhancer	68F	Spermidine synthase (CG17155); insertion is 3 kb from gene
I	85	Lethal	Enhancer	61D	Casein kinase I
J	83	60	BS	88A	Zinc-finger protein with tudor domains
L	63	0	Enhancer	86D	CG4800 similar to translationally controlled tumor protein
M	40	0	Enhancer	75C	CG12477
N	87	Lethal	Enhancer	90D	RNA-binding protein; insertion in promoter
O	78	10	BS	41C	No obvious gene candidate

P elements were mobilized by dysgenesis in a *sda*/+ genetic background. Flies were tested for behavioral paralysis following mechanical (bang) stimulation and mutant lines selected on the basis of enhanced BS paralysis, that is, on the number of flies that paralyzed in the line [listed as "Paralysis *sda*/+ (%)"]. As indicated, some mutations (A, D, F, J, and O) caused BS paralysis when separated from the *sda*/+ background [listed as "Paralysis BS (%)"]. Transposon map positions were determined by *in situ* hybridization to polytene chromosomes. In each case, genomic DNA sequences flanking the *P*-element insertion site were sequenced. Listed are candidate genes that contain or are close to the transposon insertion site.

seizure sensitivity. One possibility is suggested by its involvement in mammalian neuropeptide processing and degradation (Solhonne *et al.* 1987; Zini *et al.* 1996; Montiel *et al.* 1997; Terenius *et al.* 2000). Neuropeptides have not, thus far, been widely implicated in epilepsy, although a knockout mutation of neuropeptide Y has led to epileptic phenotypes in the mouse (Barban *et al.* 1997). Another possibility is suggested by APN involvement in malignant neoplasms (Saiki *et al.* 1993; Kido *et al.* 1999; Ishii *et al.* 2001). Tumor-cell invasion is a complex process involving cell adhesion, motility, and degradation of tissue and extracellular matrix barriers. This process resembles neuronal cell migration and growth cone outgrowth that have been implicated in epileptic syndromes in human and mouse (for example, see Aigner *et al.* 1995; Eksioglu *et al.* 1996; Fox *et al.* 1998).

An especially interesting possibility for how APN might act to alter nervous system excitability comes from a recent report implicating APN in Ca^{2+}-mediated signal transduction in monocytes (Santos *et al.* 2000). Anti-APN mAbs that inhibit enzyme activity induced a transient rise in intracellular Ca^{2+} when incubated with monocytes. The Ca^{2+} increase begins at ~30 sec and peaks at ~60 sec. A Ca^{2+} increase was not observed with control anti-APN mAbs that did not inhibit enzyme activity or with mAbs that are directed against another myeloid marker (CD33). Subsequent experiments showed that the increase arose from two separate Ca^{2+} sources. An early response was due to release from intracellular Ca^{2+} stores, possibly the sarcoplasmic reticulum; a more sustained Ca^{2+} response was due to an influx of external Ca^{2+}. Tyrosine kinase inhibitors were able to inhibit the rise in Ca^{2+} induced by ligation of APN, as were inhibitors of the phosphatidylinositol 3-kinase. It was suggested that normally *in vivo* peptides, as yet unidentified, act as ectopeptidase ligands to cause signal transduction directly via APN.

Although a similar function in brain APN has not been described yet, a parallel in epilepsy investigations shows an important role for Ca^{2+} signaling. Spontaneous mutations in mouse at the *tottering*, *lethargic*, and *stargazer* loci have each been shown to cause generalized absence epilepsy and cortical spike-wave discharges. The *tottering* locus has been shown to encode a Ca^{2+} channel α-subunit (Fletcher *et al.* 1996); the *lethargic* locus encodes a Ca^{2+} channel β-subunit (Burgess *et al.* 1997); and *stargazer* encodes a Ca^{2+} channel γ-subunit (Letts *et al.* 1998). In addition to Ca^{2+} channels, Ca^{2+} signaling appears to contribute to epilepsy syndromes in other ways. For example, seizure phenotypes are observed in a

mouse knockout mutation affecting calcium calmodulin kinase α-subunit (Butler *et al.* 1995). Mutations in synapsin I and synapsin II, molecules that mediate Ca^{2+}-dependent synaptic vesicle release, also cause seizure phenotypes (Rosahl *et al.* 1995). Also interesting are knockout mutations in mouse inositol 1,4,5-trisphosphate receptors that cause seizures and in the tyrosine kinase receptors that suppress seizures (Cain *et al.* 1995; Matsumoto *et al.* 1995).

Drosophila BS mutants: Genetic and molecular analysis of Drosophila behavioral mutants has been an effective way to identify molecules regulating nervous system excitability, such as ion channel genes (Wu and Ganetzky 1992). It is thought that knowledge gained from the Drosophila nervous system can be applied to the study of mammalian nervous system function and pathology. The underlying assumption is that even though there are differences between insect and mammalian nervous systems at the gross anatomical level, many of the fundamental cellular and molecular mechanisms regulating excitability are conserved (Benzer 1971). A further assumption is that these fundamental mechanisms, when altered by mutation, become manifest as behavioral phenotypes. Studies of *Shaker* behavioral mutants and their resulting identification and analysis of potassium channels, for instance, have given support to this notion (Kamb *et al.* 1987; Tseng-Crank *et al.* 1990).

One class of Drosophila behavioral mutants, the BS mutant class, has not been studied extensively although its behavioral and electrophysiological defects are particularly intriguing. The BS mutants have enhanced seizure sensitivity, and by studying them we may increase our understanding of what influences seizure susceptibility, a central issue in such prominent maladies as human epilepsy (McNamara 1994). A mutant screen has been described here that uses *sda*/+ heterozygous mutants as a sensitized genetic background for the isolation of new BS mutations, a procedure that is quite difficult in wild-type backgrounds. Preliminary results from this screen show that it is very efficient in identifying BS mutations using *P* elements as mutagen. Our expectation is that with other mutagens such as ethyl methanesulfonate results might even be more spectacular since such agents can sample the genome more impartially for mutations that can cause seizure sensitivity.

In conclusion, we feel that there are several unique advantages in using the Drosophila BS mutants to study seizure susceptibility. First, the BS mutants can be used in conjunction with a diverse selection of other Drosophila excitability and behavioral mutants to examine the types of molecular defects that can suppress or enhance seizure susceptibility. In addition, many excellent methodologies are available for Drosophila, such as *P*-element-mediated cloning as well as the use of the completed fly genome database, to aid in the molecular characterization of seizure sensitivity. Finally, we have developed useful electrophysiology protocols for quantifying seizures and paralysis, using the adult GF pathway (Tanouye and Wyman 1980; Pavlidis and Tanouye 1995; Kuebler and Tanouye 2000). This allows us to evaluate and compare different mutations and their combinatorial effects on seizure susceptibility. Together, these conditions make the BS mutants an attractive model with which to study seizure susceptibility.

Conclusion: The results in this article provide the first evidence that an aminopeptidase can influence the seizure susceptibility of Drosophila. We have shown here that the bang-sensitive mutant *sda*, when stimulated either mechanically or electrically can experience hyperactivity alternated with paralysis. Using various genetic and molecular analyses, we have revealed that *sda* mutants have a lesion in an aminopeptidase gene that leads directly to a drastic increase in seizure sensitivity. In future studies it would be interesting to analyze biochemically the function of this particular aminopeptidase, other molecules it may interact with, and the mechanisms by which it influences seizure sensitivity.

We thank Diana Ho for assistance in maintenance of Drosophila stocks, Tim Tully for generously providing the $sda^{iso7.8}$ allele, and John Ngai's lab for use and assistance of their cryostat apparatus. We also thank members of the Tanouye lab and others for comments on the manuscript and contributions to this work, especially Charlie Oh, Jeremy Lee, Daria Hekmat-Scafe, Xiaoyun Ren, Ed Glasscock, Aaron Yeow, Robert Newman, and David Bentley. This work was supported by a National Institutes of Health (NIH) research grant and an Epilepsy Foundation grant to M.T., an NIH postdoctoral fellowship to H.Z., and a National Science Foundation predoctoral fellowship to J.T.

LITERATURE CITED

Aigner, L., S. Arber, J. P. Kapfhammer, T. Laux, C. Schneider *et al.*, 1995 Overexpression of the neural growth-associated protein GAP-43 induces nerve sprouting in the adult nervous system of transgenic mice. Cell **83:** 269–278.

Amoscato, A., J. Alexander and G. Babcock, 1989 Surface aminopeptidase activity of human lymphocytes. I. Biochemical and biologic properties of intact cells. J. Immunol. **142:** 1245–1252.

Barban, S., G. Hollopeter, J. Erickson, P. Schwartzkroin and R. Palmiter, 1997 Knock-out mice reveal a critical antiepileptic role for neuropeptide Y. J. Neurosci. **17:** 8927–8936.

Benzer, S., 1971 From the gene to behavior. J. Am. Med. Assoc. **218:** 1015–1022.

Burgess, D., J. Jones, M. Meisler and J. Noebels, 1997 Mutation of the Ca^{2+} channel β-subunit gene Cchb4 is associated with ataxia and seizures in the *lethargic* (*lh*) mouse. Cell **88:** 385–392.

Butler, L., A. Silva, A. Abeliovich, Y. Watanabe, S. Tonegawa *et al.*, 1995 Limbic epilepsy in transgenic mice carrying a Ca^{2+}/calmodulin-dependent kinase II alpha-subunit mutation. Proc. Natl. Acad. Sci. USA **92:** 6852–6855.

Cadel, S., T. Foulon, A. Viron, A. Balogh, S. Midol-Monnet *et al.*, 1997 Aminopeptidase B from the rat testis is a bifunctional enzyme structurally related to leukotriene-A4 hydrolase. Proc. Natl. Acad. Sci. USA **94:** 2963–2968.

Cain, D., S. Grant, D. Saucier, E. Hargreaves and E. Kandel, 1995 Fyn tyrosine kinase is required for normal amygdala kindling. Epilepsy Res. **22:** 215–224.

Carthew, R., 2001 Gene silencing by double-stranded RNA. Curr. Opin. Cell Biol. **13:** 244–248.

Constam, D., A. Tobler, A. Rensing-Ehl, I. Kemler, L. Hersh *et al.*, 1995 Puromycin-sensitive aminopeptidase. Sequence analysis, expression, and functional characterization. J. Biol. Chem. **270:** 26931–26939.

Delmas, B., J. Gelfi, R. L'haridon, L. Vogel, S. Sjostrom *et al.*, 1992

Aminopeptidase N is a major receptor for the enteropathogenic coronavirus TGEV. Nature **357:** 417–420.

Delmas, B., J. Gelfi, E. Kut, H. Sjoestroem, O. Noren *et al.*, 1994 Determinants essential for the transmissible gastroenteritis virus-receptor interaction reside within a domain of aminopeptidase-N that is distinct from the enzymic site. J. Virol. **68:** 5216–5224.

Eksioglu, Y. Z., I. E. Scheffer, P. Cardenas, J. Knoll, F. DiMario *et al.*, 1996 Periventricular heterotopia: an X-linked dominant epilepsy locus causing aberrant cerebral cortical development. Neuron **16:** 77–87.

Falk, K., O. Rotzschke, S. Stevanovic and G. Jung, 1994 Pool sequencing of natural HLA-DR, -DQ, and -DP ligands reveals detailed peptide motifs, constraints of processing, and general rules. Immunogenetics **39:** 230–242.

Fletcher, C., C. Lutz, T. O'Sullivan, J. Shaughnessy, R. Hawkes *et al.*, 1996 Absence epilepsy in tottering mutant mice is associated with calcium channel defects. Cell **87:** 607–617.

Fox, J. W., E. D. Lamperti, Y. Z. Eksioglu, S. E. Hong, Y. Feng *et al.*, 1998 Mutations in *filamin 1* prevent migration of cerebral cortical neurons in human periventricular heterotopia. Neuron **21:** 1315–1325.

Fukasawa, K., K. M. Fukasawa, M. Kanai, S. Fujii and M. Harada, 1996 Molecular cloning and expression of rat liver aminopeptidase B. J. Biol. Chem. **271:** 30731–30735.

Funk, C., O. Radmark, J. Fu, T. Matsumoto, H. Jornvall *et al.*, 1987 Molecular cloning and amino acid sequence of leukotriene A4 hydrolase. Proc. Natl. Acad. Sci. USA **84:** 6677–6681.

Ganetzky, B., and C.-F. Wu, 1982 Indirect suppression involving behavioral mutants with altered nerve excitability in *Drosophila melanogaster*. Genetics **100:** 597–614.

Ishii, K., S. Usui, Y. Sugimura, S. Yoshida, T. Hioko *et al.*, 2001 Aminopeptidase N regulated by zinc in human prostate participates in tumor cell invasion. Int. J. Cancer **92:** 49–54.

Kamb, A., L. Iverson and M. Tanouye, 1987 Molecular characterization of *Shaker*, a Drosophila gene that encodes a potassium channel. Cell **50:** 405–413.

Keller, S., H. Scott, C. Mastick, R. Aebersold and G. Lienhard, 1995 Cloning and characterization of a novel insulin-regulated membrane aminopeptidase from Glut4 vesicles. J. Biol. Chem. **270:** 23612–23618.

Kennerdell, J., and R. Carthew, 1998 Use of dsRNA-mediated genetic interference to demonstrate that frizzled and frizzled 2 act in the wingless pathway. Cell **95:** 1017–1026.

Kido, A., S. Krueger, C. Haeckel and A. Roessner, 1999 Possible contribution of aminopeptidase N (APN/CD13) to invasive potential enhanced by interleukin-6 and soluble interleukin-6 receptor in human osteosarcoma cell lines. Clin. Exp. Metastasis **17:** 857–863.

Koch, A., J. Burrows, A. Skoutelis, R. Marder, P. Domer *et al.*, 1991 Monoclonal antibodies detect monocyte/macrophage activation and differentiation antigens and identify functionally distinct subpopulations of human rheumatoid synovial tissue macrophages. Am. J. Pathol. **138:** 165–173.

Kopczynski, C., J. Noordermeer, T. Serano, W. Chen, J. Pendleton *et al.*, 1998 A high thoroughput screen to identify secreted and transmembrane proteins involved in Drosophila embryogenesis. Proc. Natl. Acad. Sci. USA **95:** 9973–9978.

Kuebler, D., and M. Tanouye, 2000 Modifications of seizure susceptibility in Drosophila. J. Neurophysiol. **83:** 998–1009.

Kuebler, D., H. Zhang, X. Ren and M. Tanouye, 2001 Genetic suppression of seizure susceptibility in *Drosophila*. J. Neurophysiol. **86:** 1211–1225.

Letts, V., R. Felix, G. Biddlecome, J. Arikkath, C. Mahaffey *et al.*, 1998 The mouse *stargazer* gene encodes a neuronal Ca^{2+}-channel γ-subunit. Nat. Genet. **19:** 340–347.

Look, A., R. Ashmun, L. Shapiro and S. Peiper, 1989 Human myeloid plasma membrane glycoprotein CD13 (gp150) is identical to aminopeptidase N. J. Clin. Invest. **83:** 1299–1307.

Luciani, N., C. Marie-Claire, E. Ruffet, A. Beaumont, B. Roques *et al.*, 1998 Characterization of Glu^{350} as a critical residue involved in the N-terminal amine binding site of aminopeptidase N (EC 3.4.11.2): insights into its mechanism of action. Biochemistry **37:** 686–692.

Massuci, J., R. Miltenburger and M. Hoffman, 1990 Pattern-specific expression of the *Drosophila decapentaplegic* gene in imaginal discs is regulated by 3′ cis-regulatory elements. Genes Dev. **4:** 2011–2023.

Matsumoto, M., T. Nakagawa, T. Inoue, E. Nagata, K. Tanaka *et al.*, 1995 Ataxia and epileptic seizures in mice lacking type 1 inositol 1,4,5-trisphosphate receptor. Nature **379:** 168–171.

Mazzocco, C., K. Fukasawa, A. Raymond and J. Puiroux, 2001 Purification, partial sequencing and characterization of an insect membrane dipeptidyl aminopeptidase that degrades the insect neuropeptide proctolin. Eur. J. Biochem. **268:** 4940–4949.

McCaman, M., and J. Gabe, 1986 Sequence of the promoter and 5′ coding region of pepN, and the amino-terminus of peptidase N from Escherichia coli K-12. Mol. Gen. Genet. **204:** 148–152.

McNamara, J., 1994 Cellular and molecular basis of epilepsy. J. Neurosci. **14:** 3413–3425.

Montiel, J., F. Cormille, B. Roques and F. Noble, 1997 Nociceptin/orphanin FQ metabolism: role of aminopeptidase and endopeptidase 24.15. J. Neurochem. **68:** 354–361.

Nanus, D., D. Engelstein, G. Gastl, L. Gluck, M. Vidal *et al.*, 1993 Molecular cloning of the human kidney differentiation antigen gp160: human aminopeptidase A. Proc. Natl. Acad. Sci. USA **90:** 7069–7073.

Olsen, J., G. Cowell, E. Konigshofer, E. Danielsen, J. Moller *et al.*, 1988 Complete amino acid sequence of human intestinal aminopeptidase N as deduced from cloned cDNA. FEBS Lett. **238:** 307–314.

Pavlidis, P., and M. Tanouye, 1995 Seizures and failures in the giant fiber pathway of Drosophila bang-sensitive paralytic mutants. J. Neurosci. **15:** 5810–5819.

Pavlidis, P., M. Ramaswami and M. Tanouye, 1994 The Drosophila *easily shocked* gene: a mutation in a phospholipids pathway causes seizure, neuronal failure, and paralysis. Cell **79:** 23–33.

Prokopenko, S., Y. He, Y. Lu and H. Bellen, 2000 Mutations affecting the development of the peripheral nervous system in Drosophila: a molecular screen for novel proteins. Genetics **133:** 581–592.

Rawlings, N., and A. Barrett, 1995 Families of aspartic peptidases, and those of unknown catalytic mechanism. Methods Enzymol. **248:** 105–120.

Riemann, D., A. Kehlen and J. Langner, 1999 CD13—not just a marker in leukemia typing. Immunol. Today **20:** 83–88.

Rosahl, T., D. Spillane, M. Missler, J. Herz, D. Selig *et al.*, 1995 Essential functions of synapsins I and II in synaptic vesicle regulation. Nature **375:** 488–493.

Royden, C., V. Pirrotta and L. Jan, 1987 The *tko* locus, site of a behavioral mutation in D. melanogaster, codes for a protein homologous to prokaryotic ribosomal protein S12. Cell **51:** 165–173.

Saiki, I., H. Fujii, J. Yoneda, F. Abe, M. Nakajima *et al.*, 1993 Role of aminopeptidase N (CD13) in tumor-cell invasion and extracellular matrix degradation. Int. J. Cancer **54:** 137–143.

Sambrook, J., E. Fritsch and T. Maniatis, 1989 *Molecular Cloning: A Laboratory Manual*, Ed. 2. Cold Spring Harbor Laboratory Press, Cold Spring Harbor, NY.

Sanderink, G., Y. Artur and G. Siest, 1988 Human aminopeptidases: a review of the literature. J. Clin. Biochem. **26:** 795–807.

Santos, A. N., J. Langner, M. Herrmann and D. Riemann, 2000 Aminopeptidace N/CD13 is directly linked to signal transduction pathways in monocytes. Cell. Immunol. **201:** 22–32.

Schauder, B., L. Schomburg, J. Kohrle and K. Bauer, 1991 Cloning of a cDNA encoding an ectoenzyme that degrades thyrotropin-releasing hormone. Proc. Natl. Acad. Sci. USA **91:** 9534–9538.

Shipp, M., and A. Look, 1993 Hematopoietic differentiation antigens that are membrane-associated enzymes: cutting is the key! Blood **82:** 1052–1070.

Solhonne, B., C. Gros, H. Pollard and J. Schwarz, 1987 Major localization of aminopeptidase N in rat brain. Neuroscience **22:** 225–232.

Strausberg, R., 2001 Direct submission of mouse aminopeptidase N sequence. National Institutes of Health, Mammalian Gene Collection (MGC), Cancer Genomics Office, National Cancer Institute, Bethesda, MD.

Tanouye, M., and R. Wyman, 1980 Motor outputs of the giant nerve fiber in Drosophila. J. Neurophysiol. **44:** 405–421.

Taylor, A., 1993 Aminopeptidases: structure and function. FASEB J. **7:** 290–298.

Terenius, L., J. Sandlin and T. Sakurada, 2000 Nociceptin/or-

phanin FQ metabolism and bioactive metabolites. Peptides **21:** 919–922.

Tseng-Crank, J., G. Tseng, A. Schwartz and M. Tanouye, 1990 Molecular cloning and functional expression of a potassium channel cDNA isolated from a rat cardiac library. FEBS Lett. **268:** 63–68.

Ward, P., I. Benter, L. Dick and S. Wilk, 1990 Metabolism of vasoactive peptides by plasma and purified renal aminopeptidase M. Biochem. Pharmacol. **40:** 1725–1732.

Watt, V., and H. Willard, 1990 The human aminopeptidase N gene: isolation, chromosome localization, and DNA polymorphism analysis. Hum. Genet. **85:** 651–654.

Wilson, C., R. Pearson, H. Bellen, C. O'Kane, U. Grossniklaus *et al.*, 1989 P-element-mediated enhancer detection: an efficient method for isolating and characterizing developmentally regulated genes in *Drosophila*. Genes Dev. **3:** 1301–1313.

Wu, C., and B. Ganetzky, 1992 Neurogenetic studies of ion channels in Drosophila. Ion Channels **3:** 261–314.

Yeager, C., R. Ashmun, R. Williams, C. Cardellichio, L. Shapiro *et al.*, 1992 Human aminopeptidase N is a receptor for human coronavirus 229E. Nature **357:** 420–422.

Zini, S., M. Fournie-Zaluski, E. Chauvel, B. Roques, P. Corvol *et al.*, 1996 Identification of metabolic pathways of brain angiotensin II and III using specific aminopeptidase inhibitors: predominant role of angiotensin III in the control of vasopressin release. Proc. Natl. Acad. Sci. USA **93:** 11968–11973.

Communicating editor: T. F. C. Mackay